Influence of ion implantation on the charge storage mechanism of vanadium nitride pseudocapacitive thin films

Etienne Le Calvez, Dmitri Yarekha, Laurent Fugère, Kévin Robert, Marielle Huvé, Maya Marinova, Olivier Crosnier, Christophe Lethien, Thierry Brousse

HAL Id: hal-03266225
https://hal.science/hal-03266225

Submitted on 18 Nov 2021

Contents lists available at ScienceDirect

Electrochemistry Communications

Influence of ion implantation on the charge storage mechanism of vanadium nitride pseudocapacitive thin films

Etienne Le Calvez [a,b], Dmitri Yarekha [c], Laurent Fugère [c], Kévin Robert [b,c], Marielle Huvé [d], Maya Marinova [d], Olivier Crosnier [a,b], Christophe Lethien [b,c,*], Thierry Brousse [a,b,*]

[a] Université de Nantes, CNRS, Institut des Matériaux Jean Rouxel, IMN, F-44000 Nantes, France
[b] Réseau sur le Stockage Electrochimique de l'Energie (RS2E), CNRS FR 3459, 33 rue Saint Leu, 80039 Amiens Cedex, France
[c] Institut d'Electronique, de Microélectronique et de Nanotechnologies, Université de Lille, CNRS, Centrale Lille, Université Polytechnique Hauts-de-France, UMR 8520 - IEMN, F-59000 Lille, France
[d] Unité de Catalyse et de Chimie du Solide (UCCS), Université de Lille, CNRS, Centrale Lille, Université d'Artois, UMR 8181 – UCCS, F-59000 Lille, France

ARTICLE INFO

ABSTRACT

The influence of microstructural or structural defects is seldom investigated in pseudocapacitive electrodes. Indeed, most of the synthesized materials do present defects at every scales which contribute to the improvement of the charge storage. In this study VN thin films were deposited by reactive magnetron sputtering. The as-deposited VN films were compared with similar films implanted with arsenide cations (As$^+$) with energies ranging from 20 keV up to 150 keV. The influence of the ionic implantation on the structure and microstructure of the pristine films was characterized by several techniques. The initial curing of the internal stress of as-deposited VN films observed for low implantation energies was lost with increasing implantation energy. Concomitantly, the electrochemical behaviors of the VN films were investigated. All the VN films show a pseudocapacitive behavior at 2 mV.s^{-1}. At low scan rates, the as-deposited film exhibits the highest areal capacitance (45 mF.cm^{-2}) which drastically decreases upon increasing the scan rate. Only 30% of the initial capacitance is maintained at 100 mV.s^{-1}. Despite lower capacitances at 2 mV.s^{-1}, As$^+$ implanted VN films exhibit better capacitance retention in the same conditions, i.e. up to 65% of the initial capacitance is maintained at 100 mV.s^{-1}. The contributions coming from surface and subsurface reactions have been determined which enable to propose possible origins for the changes occurring in charge storage mechanisms upon ion implantation.

1. Introduction

Since the early evidencing of RuO$_2$ electrode peculiar behavior in HClO$_4$ aqueous electrolyte [1], pseudocapacitive materials have been the topic of extensive investigations. Indeed, their capacitive-like electrochemical signatures such as rectangular shape cyclic voltammograms (CVs) are due to specific fast and reversible Faradaic surface and subsurface reactions [2] as it has also been demonstrated for MnO$_2$ [3–5], FeWO$_4$ [6] or VN [7] electrodes among others. Although the concept of pseudocapacitance has recently been challenged [8], experimental evidences plead for charge transfer at the surface of the active material particles involving transition metal redox couples [3–5]. Many

parameters seem to influence the extend of charge storage in pseudocapacitive electrodes: the amount of electroactive cations in the pristine material, the structural defects such as vacancies, the specific surface area, the particle size and shape, and many more, which makes it difficult to determine their individual influence.

One way to overcome the presence of intrinsic defects in pseudocapacitive materials is to intentionally introduce defects which can be done by ion implantation. Indeed, by selecting the dose of implanted ions (the number of ions implanted by cm^2 of material) and the implantation energy, it is possible to tune the level of defects introduce in a given compound. Although such technique is common in microelectronic, it has rarely been applied to electrode materials for

supercapacitors. Only few studies report on its use with conducting polymers [9,10] or pseudocapacitive TiO₂ nanowires array [11].

Many investigations show that vanadium nitride (VN) is pseudoca-pacitive [7,12–15]. This transition metal nitride presents a quasi-rectangular cyclic voltammogram in aqueous KOH solution. Within an appropriate potential window, between -1.0 V and -0.4 V *vs* Hg/HgO, VN can be cycled over more than 10,000 cycles with significant capac-itance retention [16]. The charge storage mechanism in VN seems to originate from hydroxide ions exchange at the interface between the oxide/oxinitride layer and the alkaline electrolyte [7,15]. Sputtered VN films show a high electronic conductivity which allows their use as both current collector and electrode for micro-supercapacitors [7,12,13]. Sputtered VN electrodes with high surface capacitance (up to 1.2F. cm^{-2}) have been recently reported owing to high surface area coming from inter-columnar and intra-columnar porous structures [17].

Apart from their practical use as efficient electrodes in micro-supercapacitors, VN thin films are interesting model electrodes for more fundamental investigations since they do not require the use of conductive additives neither polymeric binders to be electrochemically tested [7,13]. These advantages trigger our investigations of the controlled introduction of defects in VN thin film electrodes. Here we show for the first time the implantation of Arsenic cations (As$^+$) in sputtered VN films in order to create defects and determine their in-fluence on the electrochemical behavior of VN electrodes in 1 M KOH electrolyte.

2. Experimental section

2.1. Sputtering deposition of VN thin film

VN thin films were deposited by reactive magnetron sputtering (Ar/N₂) from a pure 4″ vanadium target (99.9%) using an Alliance Concept CT200 reactor. Before the deposition, the pressure was kept below 10^{-6} mbar and the target-substrate distance was fixed at 6 cm. During the thin films deposition, DC power, argon and nitrogen flow rates were fixed at 150 W, 25 sccm and 5 sccm respectively. The substrate temperature ((1 0 0) silicon wafer) was 100 °C and the deposition time was fixed at 30 min which corresponds to ~ 300 nm-thick films. Such thickness was chosen in order to keep a good electronic conductivity [13] while observing a significant implantation depth of As$^+$ ions (see below).

To generate structural defects within the sputtered VN films, Arsenic cations (As$^+$) were implanted at different energies from 20 to 150 keV with constant implantation dose of 10^{15} ions.cm^{-2} using a EATON-AXCELIS GA 3204 reactor.

Electrochemical measurements were performed in 1 M KOH aqueous electrolyte using three electrode cell. All measurements were conducted

at a temperature of 295 K. Hg/HgO was used as reference electrode and a platinum wire as the counter electrode. Nitrogen bubbling was carried out in order to eliminate dissolved O₂ from the electrolyte. VMP3 potentiostat/galvanostat (Biologic) monitored by EC-Lab software, was used for data collection.

3. Results and discussions

300 nm-thick sputtered VN films were deposited by reactive DC sputtering. They exhibit a columnar structure (Fig. 1a) which was ex-pected from the literature reports on DC sputtered transition metal nitride films as it corresponds to the T zone of Thornton structural model [15]. In this zone, DC sputtered VN thin films show a columnar micro-structure with intercolumnar porosity [7,12,13]. The depth of ion im-plantation within the films varies with energy of implanted As$^+$ cations as depicted from the simulated plots (Fig. 1b). The implantation depth does not exceed 75 nm when an energy of 150 keV was applied. How-ever, such calculation was made for a dense VN film assuming there is no porosity. In our case, the presence of intra and inter columnar porosities due to feather like microstructure suggests that a large part of the film is affected by As$^+$ implantation although the change in VN microstructure was difficult to image from transmission electron microscopy.

An indirect effect of As$^+$ implantation can be observed from X-ray diffraction patterns. All the VN films show a cubic structure (Fm3m space group) with preferential orientation along the [1 1 1] direction of the cubic lattice (Fig. 2a). However, the shape of (1 1 1) Bragg peaks of the pristine and implanted films are quite different (Fig. 2b). To explain these changes, it is important to mention that DC sputtered thin films commonly present compressive stress in Zone T of the Thornton struc-tural model [18]. This stress also generates a broadening of the full width at half maximum (FWHM) as it is observed for the pristine VN film. Curiously, the implantation of As$^+$ ions at an energy of 20 keV results in a shift of (1 1 1) peak toward lower 2θ angle while FWHM is sharpened. This can be interpreted as the release of stress and increased crystallinity of the VN film since a major change in the nitrogen stoi-chiometry is not likely to occur with such low implantation dose. It can be stated that As$^+$ implantation at 20 keV somehow "cures" the as-grown VN film. However, this positive effect of ion implantation is not main-tained above 50 keV since at such energy the (1 1 1) peak starts shifting back to higher 2θ value while FWHM is broadened, although somehow thinner than that of the pristine VN film. The FWHM exceeds that of the pristine film at 100 keV implantation energy while leading to some kind of double peak as it is observed at 150 keV. The concomitant stress in-crease is correlated with the difference of implantation depth of the different VN thin films. From a certain thickness of the material, implanted As$^+$ cations no longer cause- damages only at the surface but
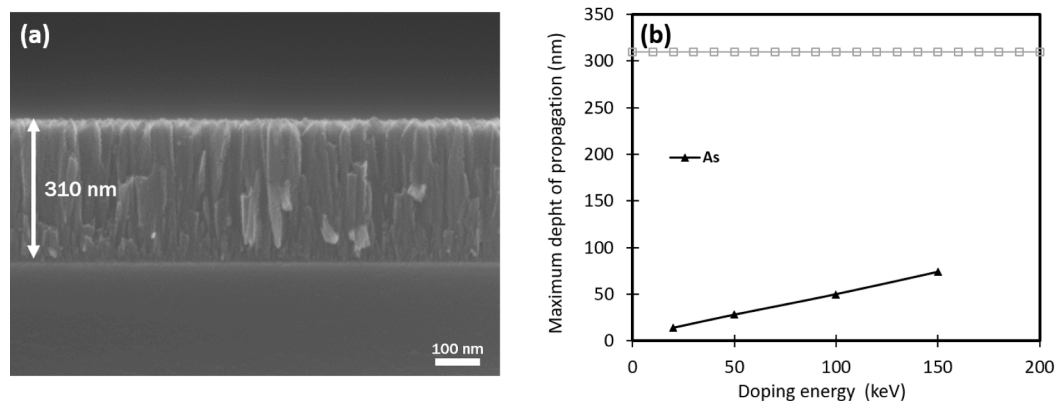

Fig. 1. (a) SEM cross-section image of as-deposited VN thin film evidencing the columnar growth. (b) Simulation of As$^+$ implantation average depth *vs* implantation energy (in keV for a dose of 10^{15} ions.cm^{-2}). The line at 310 nm represents the interface between silicon substrate and VN film. The origin of the Y axis is the upper surface of the VN film.
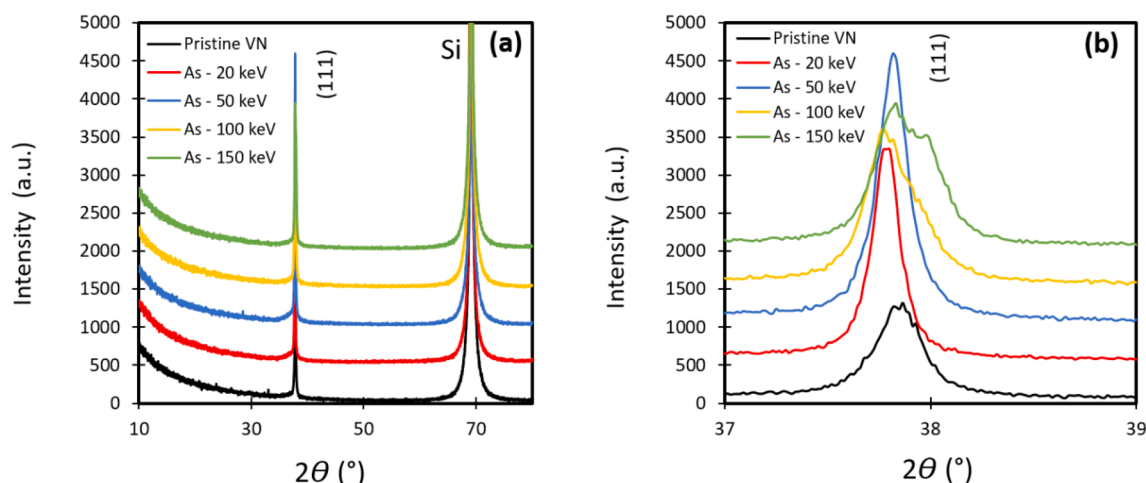
Fig. 2. (a) X-ray diffraction patterns for as-deposited and As$^+$ implanted VN films indexed in Fm3m space group (the (1 0 0) peak of silicon substrate served as reference) and (b) zoom on the Full width at half maximum (FWHM) of the (1 1 1) Bragg peak of VN for as-deposited and As$^+$ implanted VN films.

also in the bulk of the material which in turn increases internal stress.

From an electrochemical point of view, a comparison between as deposited VN film and As$^+$ implanted films is essential. Due to the small amount of implanted As$^+$ cations, their contribution to the surface capacity can be definitely ruled out. Indeed, a dose of 10^{15} ions.cm^{-2} corresponds to 0.16 mC.cm^{-2} for a one-electron process, which is less than 1% of the surface capacity of the VN films investigated in this study. Concomitantly to the observed structural changes, it seems that the effect of ion implantation significantly influences the electrochemical performance (Fig. 3). At 2 mV.s^{-1}, the CV plots of all the tested samples correspond to quasi-rectangular shape voltamperogramms (Fig. 3a). At 2 mV.s^{-1}, the highest capacitance is obtained with the pristine VN film (~47 mF.cm^{-2}, i.e. 28 mC.cm^{-2} over a 0.6 V potential window). The CV of the pristine VN film exhibits broad redox peaks superimposed to the rectangular shape envelope and centered at −0.60 V vs Hg/HgO. This pair of redox peaks is more clearly evidenced with implanted As$^+$ cations at 20 keV and 50 keV, with thinner peak width. Moreover, the peaks are shifted toward lower potential (-0.65 V vs Hg/HgO). When the implantation energy is increased up to 100 keV and more, the redox peaks are broadened again. It has been suggested that these redox peaks result from successive reductions of vanadium cation from V^{5+} to V^{2+} at the surface of vanadium nitride [15,16] and more precisely to V^{4+}/V^{3+} transition as indicated by the related Pourbaix diagram. Overall, at 2 mV.s^{-1}, the surface capacitance values decrease upon increasing the energy of implanted ions. Compared to the as-deposited VN film, nearly 30% of the capacitance measured at 2 mV.s^{-1} is lost after As$^+$ implantation at 150 keV as can be seen from Fig. 3a and d.

However, when the sweep rate is increased, the surface capacitance of pristine VN film drastically fades while much lower drop in capacitance is observed for the implanted films (Fig. 3d). At 20 mV.s^{-1}, the films implanted at 20 keV and 50 keV exhibit higher capacitance than that of as-deposited VN film (Fig. 3b). This trend is confirmed while increasing the sweep rate. At 100 mV.s^{-1}, the CV of the pristine sample looks strongly resistive (Fig. 3c) while the implanted VN electrodes still exhibit a quasi-rectangular shape with still the pair of redox peaks superimposed to the pseudocapacitive envelope. Such observation is also supported by electrochemical impedance spectroscopy experiments (Fig. 3e). The Nyquist plots of the as-deposited film is the only one to exhibit a Warburg element, thus suggesting the presence of a diffusion limited step for ions. The implanted VN thin films seem to be gathered in two groups of samples: 20–50 keV and 100–150 keV, both groups showing similar CV shapes and capacitance values. However, the first group (20–50 keV) demonstrates higher capacitance values compared to the second one which seems to indicate that there is a threshold for implantation energy over which the electrochemical performance of the

VN films are irremediably lowered.

Trasatti method [2] was used to evaluate the contribution of straightforwardly accessible surface sites, and subsurface sites that require cations diffusion to be accessed. Thus the maximum capacity (in mC.cm^{-2}) of each film can be separated in a contribution related to an "outer" surface where capacitive charge storage and redox reactions can occur without hindrance, and a contribution related to an "inner" surface where the redox reactions are quenched by the difficulty of access of cations to the redox active sites. Subsequently, Q_{outer} includes double layer charge storage and easily accessible surface redox sites, while Q_{inner} represents the surface capacity related to active sites that require cations diffusion from the electrolyte into a sub-surface layer. The different contributions, Q_{outer} and Q_{inner} capacities are plotted in Fig. 3f. The major change upon As$^+$ cation implantation is the drastic decrease of the inner component of charge storage. This goes together with the disappearance of the Warburg component upon ion implantation (Fig. 3e). Such decrease in Q_{inner} comes along with a decrease of the overall capacity of implanted films, although a large increase of the outer component is observed for all implanted films.

The Q_{outer} component is linked to the capacitive charge storage via accumulation of ions in the electrical double layer and to the pseudo-capacitive charge storage due to surface active redox site [19,20]. The implantation of ions certainly creates additional microporosity due to implanted ion tracks when they penetrate the surface of VN film. Preliminary X-ray photoelectron analyses also indicate an increase of V^{4+}/V^{3+} ratio which has recently been shown to be related to pseudocapacitance in VN films [21,22]. Thus, it is currently not easy to discriminates these two effects, but the presence of a charge transfer loop for implanted samples (Fig. 3e), that increases with implantation energy, suggests an increasing pseudocapacitive component. However, such increase in specific surface area and/or the change in vanadium mean oxidation state in oxide/oxinitride surface species seems to drastically prevent diffusion of hydroxide ion from the electrolyte to subsurface redox site according to Q_{inner} decrease. An alternative explanation could be that the structural defects introduced by implanted As$^+$ ions have created a disturbed sub-surface layer that somehow blocked the access to such "bulk" sites of VN layers. Concomitantly, it can be noted that the two implanted VN films with the largest Q_{outer}/Q_{inner} ratio, namely for 50 keV and 150 keV, exhibit the slowest capacitance fade especially at fast sweep rates (Fig. 3d). Last, the presence of redox peaks in the CVs does not seem to be related to the inner component of the capacity (Fig. 3c), thus suggesting that specific redox reactions are taking place at the surface of the films and that they are highlighted when moderate implantation energy is used (50 keV or below).
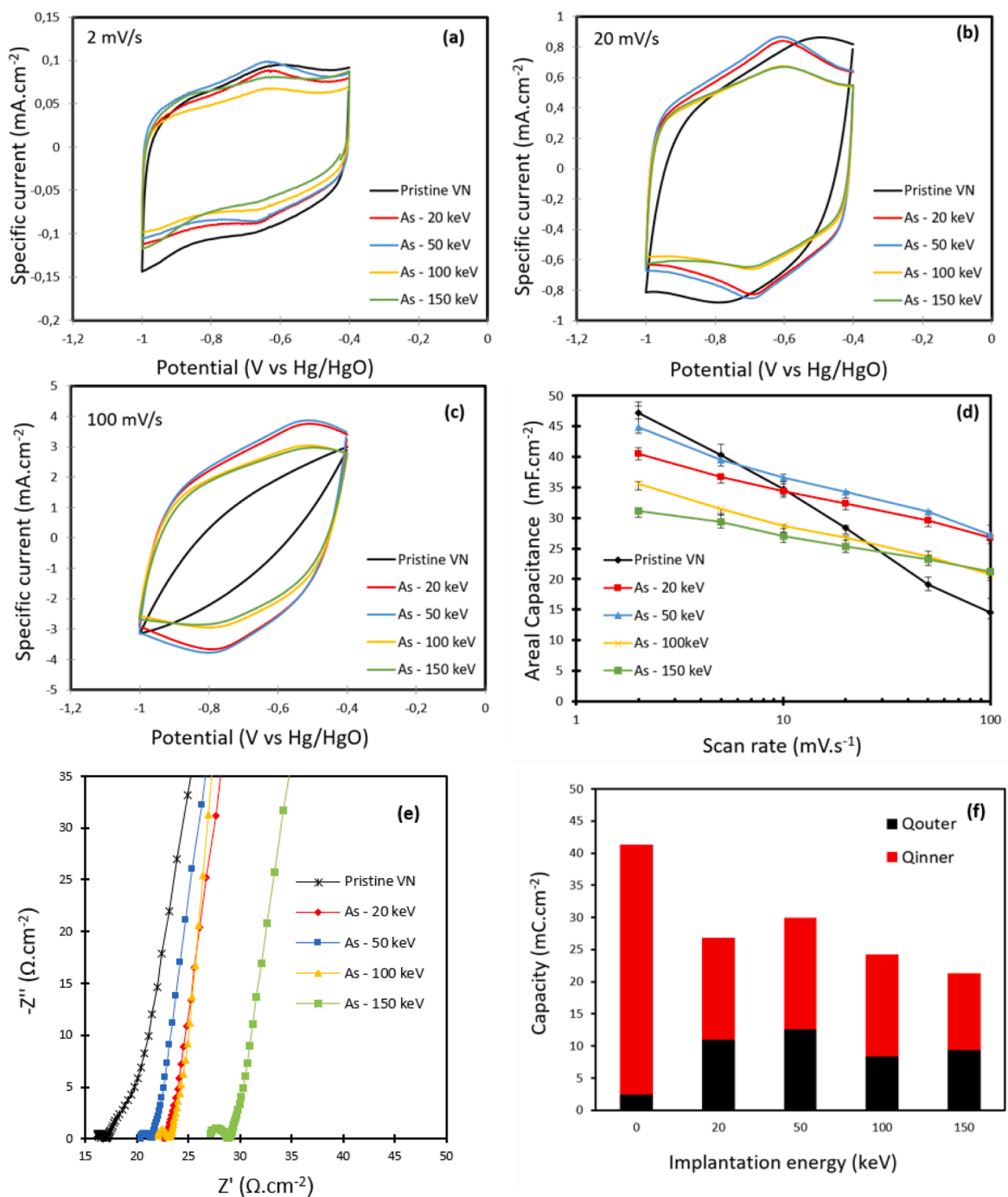
Fig. 3. CV plots of the as-deposited and As$^+$ implanted VN films at (a) 2 mV.s^{-1}, (b) 20 mV.s^{-1}, (c) 100 mV.s^{-1}. Reference electrode: Hg/HgO; counter electrode: platinum wire; electrolyte: 1 M KOH. (d) Summary of the areal capacitance values *vs* the implanted energy for VN thin films. (e) Nyquist plot of the as-deposited and As$^+$ implanted VN films. (f) Deconvolution of outer and inner surface capacity for the as-deposited VN thin film and the As$^+$ implanted ones (determination of Q$_{inner}$ and Q$_{outer}$ was performed according to ref. [2]).

4. Conclusion

In this communication, we evidenced for the first time the role of implanted ions in the charge storage mechanism of pseudocapacitive VN films, especially with regard to the implantation energy. As$^+$ implantation leads to drastic changes in the overall capacitance of the VN thin film electrodes. These changes are related to an immediate fade in the inner capacity whatever the implantation energy, while the outer capacity component related to capacitive or/and pseudocapacitive surface processes is emphasized upon ion implantation. Although further work is required to pertinently discriminate the role of intentionally implanted defects, especially on denser films, such methodology could be further used for highlighting the role of defects in pseudocapacitive materials such as FeWO$_4$.

CRediT authorship contribution statement

Etienne Le Calvez: Investigation, Methodology, Writing - review & editing. **Dmitri Yarekha:** Investigation. **Laurent Fugère:** Investigation. **Kévin Robert:** Investigation. **Marielle Huvé:** Investigation. **Maya Marinova:** Investigation. **Olivier Crosnier:** Conceptualization, Methodology, Supervision, Writing - review & editing. **Christophe Lethien:**

Conceptualization, Methodology, Supervision, Writing - review & editing. **Thierry Brousse:** Conceptualization, Methodology, Supervision, Writing - review & editing.

Declaration of Competing Interest

The authors declare that they have no known competing financial interests or personal relationships that could have appeared to influence the work reported in this paper.

Acknowledgement

References

[1] S. Trasatti, G. Buzzanca, Ruthenium dioxide: a new interesting electrode material, Solid state structure and electrochemical behavior, J. Electroanal. Chem. 29 (1971) A1–A5, https://doi.org/10.1016/S0022-0728(71)80111-0.

[2] S. Ardizzone, G. Fregonara, S. Trasatti, "Inner" and "Outer" Active Surface of RuO2 Electrodes, Electrochimica Acta. 35 (1) (1990) 263–267, https://doi.org/10.1016/0013-4686(90)85068-X.

[3] M. Toupin, T. Brousse, D. Bélanger, Charge Storage Mechanism of MnO2 Electrode Used in Aqueous Electrochemical Capacitor, Chem. Mater. 16 (16) (2004) 3184–3190, https://doi.org/10.1021/cm049649j.

[4] J.-K. Chang, M.-T. Lee, W.-T. Tsai, In situ Mn K-edge X-ray absorption spectroscopic studies of anodically deposited manganese oxide with relevance to supercapacitor applications, J. Power Sources. 166 (2) (2007) 590–594, https://doi.org/10.1016/j.jpowsour.2007.01.036.

[5] K.-W. Nam, M.G. Kim, K.-B. Kim, In Situ Mn K-edge X-ray Absorption Spectroscopy Studies of Electrodeposited Manganese Oxide Films for Electrochemical Capacitors, J. Phys. Chem. C. 111 (2) (2007) 749–758, https://doi.org/10.1021/jp063130o.

[6] N. Goubard-Bretesché, O. Crosnier, C. Douard, A. Iadecola, R. Retoux, C. Payen, M.-L. Doublet, K. Kisu, E. Iwama, K. Naoi, F. Favier, T. Brousse, Unveiling Pseudocapacitive Charge Storage Behavior in FeWO4 Electrode Material by Operando X-Ray Absorption Spectroscopy, Small. 16 (33) (2020) 2002855, https://doi.org/10.1002/smll.202002855.

[7] K. Robert, D. Stiévenard, D. Deresmes, C. Douard, A. Iadecola, D. Troadec, P. Simon, N. Nuns, M. Marinova, M. Huvé, P. Roussel, T. Brousse, C. Lethien, Novel Insights into the Charge Storage Mechanism in Pseudocapacitive Vanadium Nitride Thick Films for High-Performance on-Chip Micro-Supercapacitors, Energy Environ. Sci. 13 (3) (2020) 949–957, https://doi.org/10.1039/C9EE03787J.

[8] C. Costentin, J.-M. Savéant, Energy Storage: pseudocapacitance in prospect, Chem. Sci. 10 (22) (2019) 5656–5666, https://doi.org/10.1039/C9SC01662G.

[9] A.M.P. Hussain, D. Saikia, F. Singh, D.K. Avasthi, A. Kumar, Effects of 160 MeV Ni^{12+} ion irradiation on polypyrrole conducting polymer electrode materials for all polymer redox supercapacitor, Nuclear Instrum. Methods Phys. Res. B 240 (4) (2005) 834–841, https://doi.org/10.1016/j.nimb.2005.06.204.

[10] A.M.P. Hussain, A. Kumar, Enhanced electrochemical stability of all-polymer redox supercapacitors with modified polypyrrole electrodes, J. Power Sources 161 (2) (2006) 1486–1492, https://doi.org/10.1016/j.jpowsour.2006.05.051.

[11] J. Cui, L. Cao, D. Zeng, X. Wang, W. Li, Z. Lin, P. Zhang, Surface Characteristic Effect of Ag/TiO$_2$ Nanoarray Composite Structure on Supercapacitor Electrode Properties, Scanning 2018 (2018) 1–10, https://doi.org/10.1155/2018/2464981.

[12] R. Lucio-Porto, S. Bouhtiyya, J.F. Pierson, A. Morel, F. Capon, P. Boulet, T. Brousse, VN Thin Films as Electrode Materials for Electrochemical Capacitors, Electrochimica Acta. 141 (2014) 203–211, https://doi.org/10.1016/j.electacta.2014.07.056.

[13] K. Robert, C. Douard, A. Demortière, F. Blanchard, P. Roussel, T. Brousse, C. Lethien, On Chip Interdigitated Micro-Supercapacitors Based on Sputtered Bifunctional Vanadium Nitride Thin Films with Finely Tuned Inter- and Intracolumnar Porosities, Adv. Mater. Technol. 3 (7) (2018) 1800036, https://doi.org/10.1002/admt.201800036.

[14] X. Lu, M. Yu, T. Zhai, G. Wang, S. Xie, T. Liu, C. Liang, Y. Tong, Y. Li, High Energy Density Asymmetric Quasi-Solid-State Supercapacitor Based on Porous Vanadium Nitride Nanowire Anode, Nano Lett. 13 (6) (2013) 2628–2633, https://doi.org/10.1021/nl400760a.

[15] D. Choi, G.E. Blomgren, P.N. Kumta, Fast and Reversible Surface Redox Reaction in Nanocrystalline Vanadium Nitride Supercapacitors, Adv. Mater. 18 (9) (2006) 1178–1182, https://doi.org/10.1002/adma.v18:910.1002/adma.200502471.

[16] A. Morel, Y. Borjon-Piron, R.L. Porto, T. Brousse, D. Bélanger, Suitable Conditions for the Use of Vanadium Nitride as an Electrode for Electrochemical Capacitor, J. Electrochem. Soc. 163 (6) (2016) A1077–A1082, https://doi.org/10.1149/2.1221606jes.

[17] C. Lethien, J. Le Bideau, T. Brousse, Challenges and Prospects of 3D Micro-Supercapacitors for Powering the Internet of Things, Energy Environ. Sci. 12 (1) (2019) 96–115, https://doi.org/10.1039/C8EE02029A.

[18] J.A. Thornton, The Microstructure of Sputter-deposited Coatings, J. Vac. Sci. Technol. A 4 (6) (1986) 3059–3065, https://doi.org/10.1116/1.573628.

[19] T. Brousse, D. Bélanger, J.W. Long, To Be or Not To Be Pseudocapacitive? J. Electrochem. Soc. 162 (5) (2015) A5185–A5189, https://doi.org/10.1149/2.0201505jes.

[20] B.E. Conway, Transition from "Supercapacitor" to "Battery" Behavior in Electrochemical Energy Storage, J. Electrochem. Soc. 138 (6) (1991) 1539–1548, https://doi.org/10.1149/1.2085829.

[21] Y. Liu, L. Liu, L. Kang, F. Ran, Vanadium Nitride with Surface Single Specie Oxide via Vanadium-Organic Frameworks Precursor, J. Power Sources. 450 (2020) 227687, https://doi.org/10.1016/j.jpowsour.2019.227687.

[22] B.o. Chen, L. Han, B. Li, Pseudo-Capacitance Behaviour of Reactively Sputtered Vanadium Nitride Electrodes Deposited at Different Working Pressures: The Critical Role of Surface Chemistry, Mater. Chem. Phys. 236 (2019) 121820, https://doi.org/10.1016/j.matchemphys.2019.121820.